Sirius RF Plant Identification and Control

Keywords: *LLRF; Control Engineering; System Identification.*

D. Daminelli*[1,2], F. K. G. Hoshino[1], A. P. B. Lima[1], M. Souza (advisor)[2]

[1]Brazilian Synchrotron Light Laboratory, Campinas, Brazil

[2]University of Campinas, Campinas, Brazil

Abstract

Resonant Cavities are devices present in particle accelerators such as Sirius, which aim to compensate energy losses of the electron beam, caused by radiation emissions in the accelerator, through an electromagnetic field generated from a Radio Frequency (RF) signal, which must have its amplitude and phase precisely controlled to perform its function as desired. Optimizations are needed to achieve the best performance. Therefore, System Identification techniques can be used to model the plant and find the parameters that best tune the controller. This report presents the results of the study performed to identify and improve the control parameters of the Sirius RF Plant, where a 95% fit model could be achieved and initial test with new parameters for the controller were promising to enhance the system's disturbance rejection in closed loop operation.

1 Introduction

Sirius is a Synchrotron Light Source currently operating in Campinas, São Paulo State, Brazil [1]. Synchrotron Light Sources are a category of particle accelerators in which electromagnetic fields are used to accelerate well-defined beams of electrically-charged particles to high energies. The beam path is then bent by some special magnets to generate the Synchrotron Radiation, which is used in science research such as the study of atomic structure, medicine, biology, chemistry, crystallography and many other applications [2].

To increase and maintain the beam energy, Radio Frequency (RF) Cavities are used – metallic structures under vacuum where electromagnetic fields oscillating with a frequency of a few hundred of MHz will interact with the electron beam.

To be properly accelerated, particles must see a certain amplitude and phase of the electric field. The Low-Level RF (LLRF), a low-power closed loop control system, is responsible to ensure these conditions.

---

*david.daminelli@cnpem.br

Until now, the Sirius LLRF controller parameters were tuned with a pragmatic approach to ensure beam stability. In order to optimize these parameters, improving output disturbance rejection, and mitigate longitudinal instabilities [3], a study has been conducted to identify the RF plant and find a parametric polynomial model that can be used along with MATLAB's Control Toolbox[4] to fine tune the PI loop. The methods and results of this study are discussed in the following sections.

1.1 Sirius RF Plant

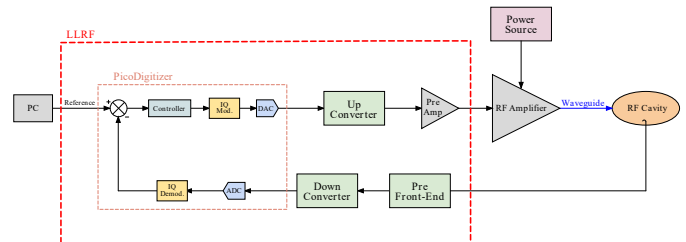Figure 1 shows a block diagram from the Sirius RF System.

Figure 1: Sirius RF Plant block diagram.

Sirius LLRF [5] is a digital system designed to achieve 0.1 % amplitude and 0.1° phase stability under normal operating conditions [6, 7].

The main digital signal processing unit is the PicoDigitizer from Nutaq [8], which houses the Xilinx Virtex-6 SX315T Field Programmable Gate Array (FPGA) and two FPGA Mezzanine Card (FMC) boards: a 16-channel 14-bit 125 MSPS Analog-to-Digital Converter (ADC) board and a 8-channel 16-bit 250 MSPS Digital-to-Analog Converter (DAC) board.

Regarding the many features available in LLRF, some were particularly useful for this study:

- IQ Digital Modulation/Demodulation

- PI Loops for Cavity Voltage Control in IQ (rectangular) or Polar loops

- Phase Shifters and Gain control on each DAC's outpus and ADC's Input
- Fast Data Logger (FDL) for fast data acquisition and post-mortem analysis
- Conditioning mode with a 10 Hz square-modulated RF Drive output.

1.2 Linear Models

System identification refers to the general process of extracting information about a system from measured input-output data [9]. There are multiple ways of representing a system, but some are especially suitable for system identification, as they are based on well-established algorithms [10].

Parametric Polynomial Models

In this study, linear discrete representations fits well for this application. A general discrete model can be written as follows:

$$y(k) = \frac{B(q)}{A(q)F(q)}u(k) + \frac{C(q)}{A(q)D(q)}\nu(k), \qquad (1)$$

with q being the delay operator, that is $y(k)q^{-1} = y(k-1)$, $\nu(k)$ a white Gaussian noise and $A(q)$, $B(q)$, $C(q)$, $D(q)$, and $F(q)$ the following polynomials:

$$
\begin{aligned}
A(q) &= 1 - a_1 q^{-1} - \cdots - a_{n_y} q^{-n_y} \\
B(q) &= b_1 q^{-1} + \cdots + b_{n_u} q^{-n_u} \\
C(q) &= 1 + c_1 q^{-1} + \cdots + c_{n_v} q^{-n_v} \qquad (2) \\
D(q) &= 1 + d_1 q^{-1} + \cdots + d_{n_d} q^{-n_d} \\
F(q) &= 1 + f_1 q^{-1} + \cdots + f_{f_v} q^{-f_v}.
\end{aligned}
$$

From the generic model shown in (1) we can obtain simpler models useful for the identification of several types of systems. For this study, an Output Error model, shown in Eq. (3) was chosen to describe the RF Plant, as it was assumed that the noise was a white Gaussian noise and added directly to the output, without being filtered by the plant:

$$y(k) = \frac{B(q)}{F(q)}u(k) + \nu(k). \qquad (3)$$

1.3 IQ Demodulation

Sirius's LLRF is based on an IQ modulation/demodulation technique. A signal $x(t)$ centered on a carrier at ω_c rad/s can be expressed as following:

$$x(t) = x_i(t)cos(\omega_c t) - x_q(t)sin(\omega_c t), \qquad (4)$$

where $x_i(t)$ and $x_q(t)$ are, respectively, the In-Phase and Quadrature base-band envelopes.

The transmission of $x(t)$ over a system with impulse response $h(t)$ can be obtained from the convolution product:

$$y(t) = h(t) * x(t). \qquad (5)$$

From Eq. (4) and (5), analysing in base-band, we derive that[11]:

$$
\begin{bmatrix} y_i(t) \\ y_q(t) \end{bmatrix} = \begin{bmatrix} h_s(t) & h_c(t) \\ -h_c(t) & h_s(t) \end{bmatrix} * \begin{bmatrix} x_i(t) \\ x_q(t) \end{bmatrix}, \qquad (6)
$$
$$h_s(t) = h_{ii}(t) = h_{qq}(t) = h(t)cos(\omega_c t),$$
$$h_c(t) = h_{qi}(t) = -h_{iq}(t) = -h(t)sin(\omega_c t),$$

where $y_i(t)$ and $y_q(t)$ are, respectively, the output In-Phase and Quadrature base-band envelopes.

Therefore, two linear models must be found when modeling the system: one for the straight impulse response $h_s(t)$ and one for the crossed impulse response $h_c(t)$.

2 Methodology

This study can be summarized in three steps: Data acquisition and processing; System Identification; and Controller Tuning. MATLAB scripts were implemented to process the raw data and some toolboxes were used for modeling and tuning, described in detail as follow.

2.1 Data Processing

Initially, a set of data was collected from the RF plant in open loop using the FDL and Conditioning Mode. As previously demonstrated in Eq. (6), two sets of transfer functions must be modeled: a straight one, which can be obtained by driving the I input and measuring the I output (same for Q input and output), and a crossed one, which can be obtained by driving the I input and measuring the Q output (same for Q input and I output). The data obtained by driving the I input only can be seen in Fig. 2a, linearized around the operating point by subtracting its mean value. The output was measured in the cavity, acquired by the LLRF. Similarly, an equivalent data was obtained by driving Q only, in addition to other amplitude values. This set data was further used to estimation and validation.

The IQ data collected is digitized by the PicoDigitizer at a 41.6 MHz sample rate. Despite the large frequency resolution, the LLRF can only perform in a bandwidth of a few tens of kHz. Therefore, the data can be filtered and decimated without loosing useful information, thus reducing the noise and the identification algorithms runtime. Furthermore, an oscillation around 60 Hz is noticeable. A notch filter was applied to mitigate this noise. Figure 2b shows the data after the processing described previously.

2.2 System Identification

MATLAB's System Identification Toolbox [12] were used to estimate the functions and compare with validation data. This comparison can be seen in Fig. 3.
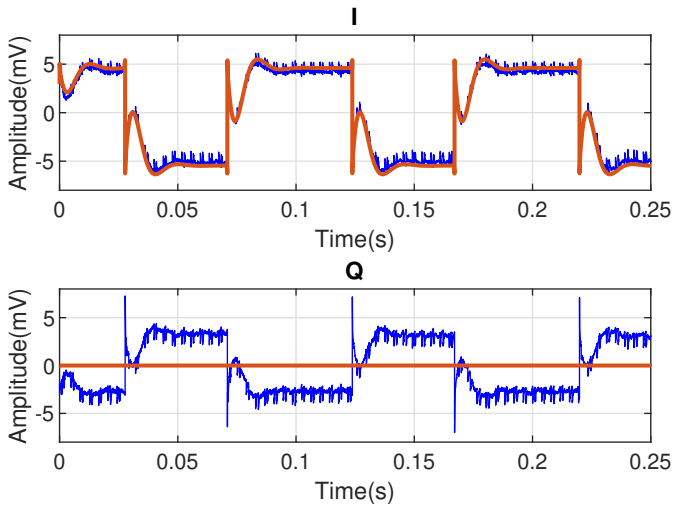
Equations (7) and (8) present, respectively, the estimated straight ($H_s(z)$) and crossed ($H_c(z)$) transfer functions.

$$H_s(z) = \frac{0.0315z^{-1} - 0.0285z^{-2}}{1 - 3.228z^{-1} + 4.068z^{-2} - 2.391z^{-3} + 0.555z^{-4}} \qquad (7)$$

$$H_c(z) = \frac{0.0778z^{-1} - 0.0765z^{-2}}{1 - 2.197z^{-1} + 1.238z^{-2} + 0.199z^{-3} - 0.238z^{-4}} \qquad (8)$$
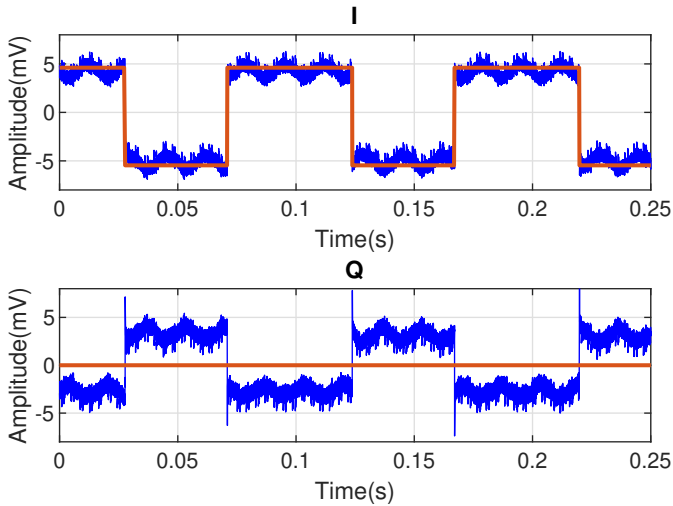
(a) Raw data

(b) Processed data

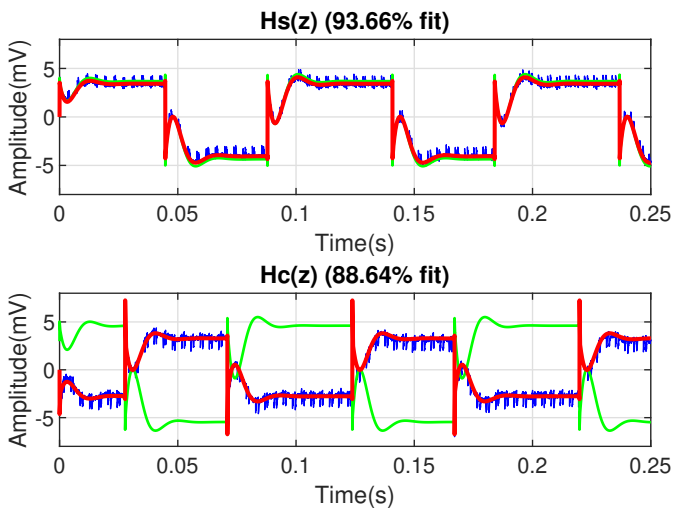Figure 2: I and Q output (blue) signals obtained by driving I input only (orange).

Figure 3: Estimated discrete models outputs (red) compared to measured validation data (blue) when driven by the same input reference signal (green).

Since the final goal is to tune the LLRF PI loop, it is convenient to have the continuous equivalent of the discrete functions and use a discrete-time equivalent design

method [13]. Equations (9) and (10) present, respectively, the estimated straight ($H_s(s)$) and crossed ($H_c(s)$) continuous transfer functions, estimated using the MATLAB's System Identification Toolbox.

$$H_s(s) =$$
$$\frac{1.271e5 \cdot s^3 + 8.89e9 \cdot s^2 + 7.231e15 \cdot s + 3.218e20}{s^4 + 2.215e5 \cdot s^3 + 6.489e10 \cdot s^2 + 9.982e15 \cdot s + 3.468e20} \quad (9)$$

$$H_c(s) =$$
$$\frac{1.373e5 \cdot s^3 + 2.819e7 \cdot s^2 + 1.944e16 \cdot s + 2.894e20}{s^4 + 2.769e5 \cdot s^3 + 1.417e11 \cdot s^2 + 1.879e16 \cdot s + 4.82e20} \quad (10)$$

Figure 4 shows the complete RF Plant model, used to obtain the comparison between the estimated continuous models shown in Fig. 5.
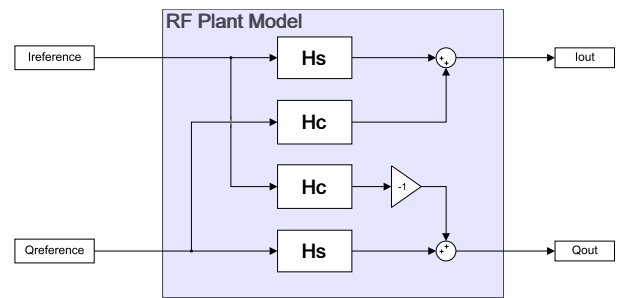

Figure 4: Simulink's block diagram of Sirius RF Plant Model in open loop.
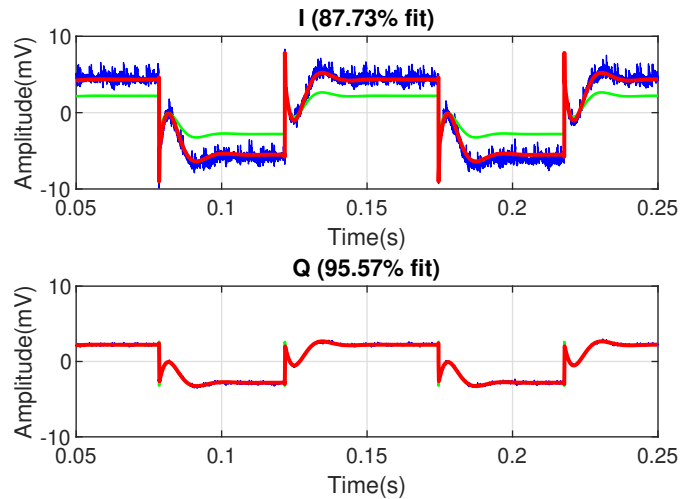

Figure 5: Estimated continuous model outputs (red) compared to measured validation data (blue) when driven by the same input reference signal (green).

2.3 Controller Tuning

Figure 6 shows the model in closed loop, as is implemented on the PicoDigitizer. The PI controller is implemented as the following:

$$PI(z) = k_p + k_i \frac{z}{z-1}, \quad (11)$$

3

where k_p is the proportional gain and k_i the integral gain. Both I and Q Controllers share the same k_p and k_i parameters.
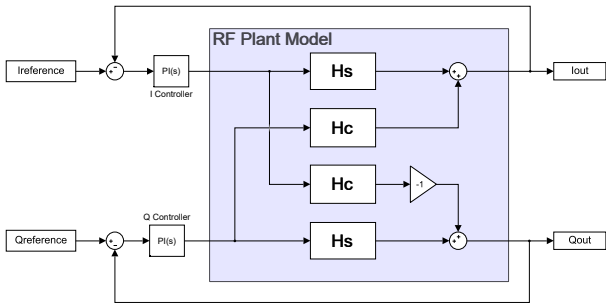

Figure 6: Simulink's block diagram of Sirius RF Plant Model in closed loop.

Using the Tustin's Method, Eq. (11) can be written as:

$$PI(s) = PI(z)|_{z=\frac{T_s s + 2}{2 - T_s s}} = k_p + \frac{k_i}{T_s} \cdot \frac{0.5 T_s s + 1}{s}, \quad (12)$$

where T_s is the sample period.

As previously shown, the model found is a Multiple Inputs Multiple Outputs (MIMO) System, and its controller's design is already established. So, it is only necessary to find the k_i and k_p parameters that satisfy the control specifications. One approach to this problem is tuning the controller considering the straight transfer function only, and then verifying if the parameters found satisfies the initial requirements for the complete model.

For the intended operation, the LLRF must mitigate output disturbances up to 2 kHz. Furthermore, due the PicoDigitizer's firmware implementation, the maximum k_i and k_p values are, respectively, $1.9531e{-}3$ and $3.906e{-}3$.

Using MATLAB's *sisotool*, the parameters $k_i = 4.172e{-}4$ and $k_p = 1.953e{-}2$ were found.

Figure 7 shows a Simulink's block diagram that was used alongside the Simulink's Bode block to plot the system Disturbance Rejection when the control parameters are the ones currently being used ($k_i = 1.788e{-}6$ and $k_p = 1.172e{-}2$) and the ones mentioned above, when considering H_s only and the complete model. Figure 8 shows this comparison, with k being the crossed function gain shown in Fig. 7.
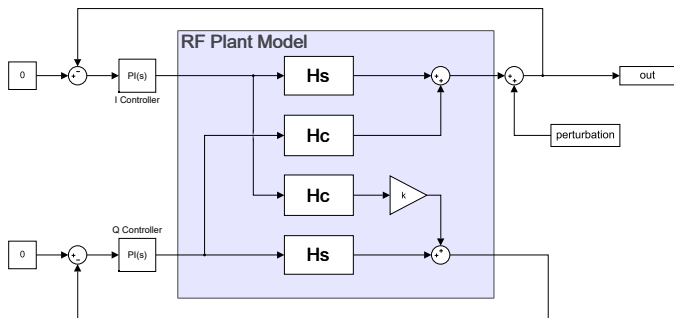

Figure 7: Simulink's Block Diagram of the RF Plant Model in closed loop with output perturbation.

Therefore, the new parameters found can mitigate output disturbances up to 6 kHz (considering 3 dB attenuation), while the parameters currently being used can only mitigate up to 20 Hz output disturbances.
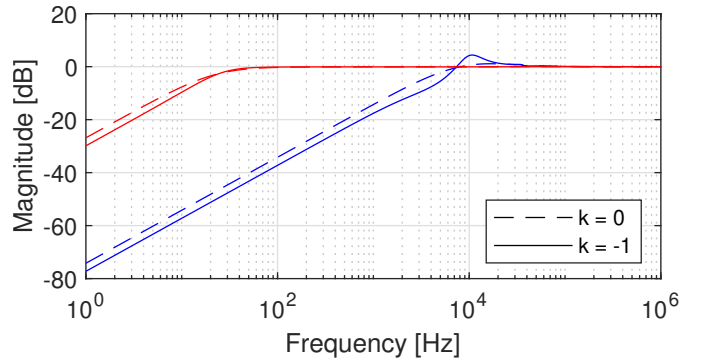

Figure 8: Disturbance Rejection with the control parameters being the currently in use (red) and the new ones found (blue), when considering H_s only (dashed) and the complete model (solid).

3 Results & Discussion

Figure 9 shows the Cavity Voltage Amplitude Spectrum, acquired by the FDL, in closed loop, without the electron beam. It is noticeable that the new parameters found were able to improve the Disturbance Rejection by mitigating noises up to 5 kHz.
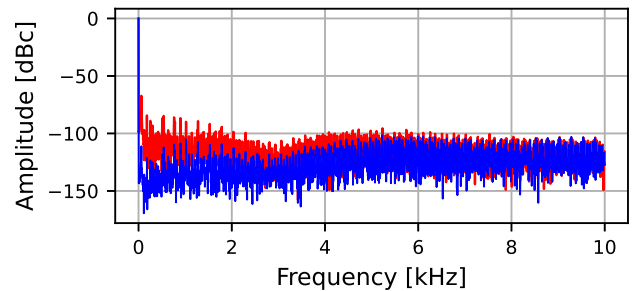

Figure 9: Cavity Voltage Amplitude Spectrum at closed loop, acquired by the FDL, with current parameters (red) and new parameters (blue)

By making use of a Spectrum Analyzer, a set of data was collected by measuring the Pre Front-End output (cf. Fig. 1). It was expected that this measurement and the FDL data (shown in Fig. 9) would show a similar result, as the RF Frond-End should not introduce any noise into the signal. However, Fig 10 shows that, with the new parameters, although the FDL shows that there has been an improvement in the entire spectrum displayed, the Spectrum Analyzer shows that there was actually a gain in the 60 Hz frequency and its odd harmonics. This indicates that the RF Front-End is indeed introducing noise into the signal, which causes the control loop, in order to compensate that noise, to end up amplifying those frequencies in the cavity.

4 Conclusion

The estimated models, despite its limitations, were able to satisfactorily describe the RF Plant dynamics around the operating point. Further studies should be conducted to better understand the LLRF components, thus refining the models and including electron beam effects.
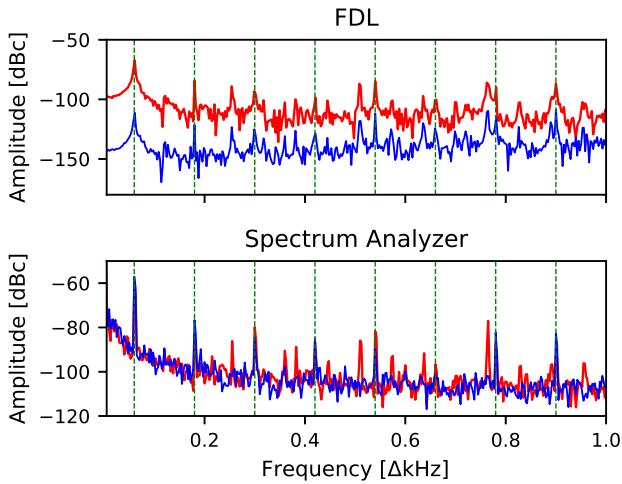
Figure 10: FDL (upper) and Spectrum Analyzer (bottom) data at closed loop with current parameters (red) and new parameters (blue), with the 60Hz odd harmonics (dashed green) indicated.

Furthermore, the control parameters found were promising to improve the system's disturbance rejection when comparing to the current parameters being used. Further studies should be conducted to find and mitigate the 60Hz noise source, thus improving this noises at the RF Cavity.

Finally, further studies should be carried out to evaluate if the parameters found were able to guarantee the beam stability while mitigating the longitudinal instabilities.

References

[1] Sirius: Accelerating the Future of Brazilian Science. https://www.lnls.cnpem.br/sirius-en/. Accessed on 07/04/2022.

[2] Hooman Hassan Zadegan. *Design, analysis and implementation of a versatile low level radio frequency system for accelerating cavities*. Servicio Editorial de la Universidad del País Vasco/Euskal Herriko Unibertsitatearen Argitalpen Zerbitzua, 2011.

[3] L. Liu, M.B. Alves, A.C.S. Oliveira, X.R. Resende, and F.H. de Sá. Sirius Commissioning Results and Operation Status. In *Proc. IPAC'21*, number 12 in International Particle Accelerator Conference, pages 13–18. JACoW Publishing, Geneva, Switzerland, 08 2021. https://doi.org/10.18429/JACoW-IPAC2021-MOXA03.

[4] Control system toolbox. https://www.mathworks.com/products/control.html.

[5] A. P. B. Lima, D. Daminelli, M. Hoffmann Wallner, F. K. G. Hoshino, I. Carvalho de Almeida, and R. H. A. Farias. Sirius Storage Ring RF System Status Update. Number 13 in International Particle Accelerator Conference. JACoW Publishing, Geneva, Switzerland. presented at IPAC'22, Bangkok, Thailand, Jun. 2022, paper TUPOST014, this conference.

[6] A. Salom, R.H.A. Farias, F.K.G. Hoshino, A.P.B. Lima, and F. Pérez. Sirius Digital LLRF. In *Proc. 10th International Particle Accelerator Conference (IPAC'19), Melbourne, Australia, 19-24 May 2019*, number 10 in International Particle Accelerator Conference, pages 4244–4247, Geneva, Switzerland, Jun. 2019. JACoW Publishing. https://doi.org/10.18429/JACoW-IPAC2019-THPTS060.

[7] A. P. B. Lima, F. K. G. Hoshino, C. F. Carneiro, R. H. A. Farias, and A. Salom. *Sirius Digital Low-Level RF Status. arXiv preprint arXiv:1910.08499*, 2019.

[8] Nutaq. https://nutaq.com/products/picodigitizer-125-series.

[9] T Schilcher. RF applications in digital signal processing. 2008.

[10] Luis Aguirre. *Introdução à Identificação de Sistemas*. Editora UFMG, 2015.

[11] R Garoby. Low level RF and feedback. page 35 p, Jun 1997.

[12] System identification toolbox. https://www.mathworks.com/products/sysid.html.

[13] Gene F Franklin, J David Powell, Abbas Emami-Naeini, and J David Powell. *Feedback control of dynamic systems*, volume 4. Prentice hall Upper Saddle River, 2002.